Astron. Astrophys. 330, 1136–1144 (1998)

ASTRONOMY
AND
ASTROPHYSICS

Solar mesogranule lifetime measurements

Th. Roudier[1], **J.M. Malherbe**[2], **J. Vigneau**[3], **and B. Pfeiffer**[3]

[1] Observatoire Midi-Pyrénées, UMR 5572 Pic du Midi, F-65201 Bagnères de Bigorre, France
[2] Observatoire de Paris, Section de Meudon, URA 2080, DASOP, F-92195 Meudon, France
[3] Observatoire Midi-Pyrénées, UMR 5572 Pic du Midi, F-31400 Toulouse, France

Received 30 April 1997 / Accepted 13 October 1997

Abstract. We present a study in which the solar lifetime of mesocells (4–10 arcsec) was determined from a long time sequence (6 h 40 min) obtained at the Pic du Midi Observatory. The mesocell detection was performed by local correlation tracking, using various spatial and temporal windows. The histograms derived from the visual measurements reveal that mesoscale lifetime is between 10 min and 160 min, with peaked distributions around 30–40 min. The indirect method for lifetime estimation using a correlation coefficient, gives a mesocale lifetime from 16 to 185 min depending on the temporal window and the methods used. The proper motions of the long-living mesocells are found to be random with respect to the superganule flows, with the peak distribution of horizontal velocities at 0.5 km/s. The results of this mesocell lifetime determination method are smaller by a factor of 2 to 5 with respect to the previous results. This difference could be attributed to the mesocell definition, the method of measurement or the different location of the mesocell field of view in the supergranular network.

Key words: Sun: photosphere – Sun: granulation – convection

1. Introduction

The solar surface is subject to convective and oscillatory motions, the properties of which are fundamental to understanding the physics of solar surface evolution. The convective motions which concentrate, sweep and spread magnetic fields over the solar surface, are the basic elements which contribute to magnetic activity in the quiet sun. A study of their physical properties needs to address many issues, such as the g-mode detection (Andersen et al. 1994), the solar background irradiance (Rabello Soarres et al. 1997), the magnetic flux tube concentration, the photospheric network formation, the measurement of the diffusion coefficients and the motions of magnetic flux tubes (cf. Coronal heating). At the present time, three different convective scales have been identified (or are suspected to exist) on the solar surface. The best known is solar granulation, followed by mesogranulation (November et al. 1981,1982) and supergranulation (Leighton et al. 1962). A rough description of the macro-properties of such cells can be given by their mean size, velocity and lifetime. The solar granulation, for example, is characterized by a mean size of 1000 km, a Doppler velocity of 1 km/s at the disk center (i.e. vertical motions), a radial expansion of 1.6 to 2.6 km/s (Brandt et al. 1991) and a lifetime of 10 to 16 min. Meanwhile, the supergranulation is generally defined by a chromospheric network (or Doppler data), with a scale of 20 to 50 Mm, a vertical velocity of 50 m/s (Küveler, 1983), a horizontal flow of 500 m/s and a lifetime of around 20 hours (Simon and Leigton, 1964). Finally, the mesogranulation has a typical scale of 5-10 Mm, a vertical velocity of 60 to 200 m/s (rms) and a horizontal velocity of 450 m/s (Deubner et al. 1989). Its lifetime has not as of yet been accurately determined. In the first determination by November et al. (1981), these mesogranules persisted for at least 2 hours but in other studies they seem to survive for at least 3 h (Muller et al 1992) which is much longer than the lifetime of exploding granules. Recently, a 1/e lifetime of 5 to 6 hours was found by Brandt et al. 1994 for mesoscale flows from a 4.5 hours image sequence. A previous determination by Darvann (1991) estimates the 1/e lifetime to lie between 3.5 to 7 hours with a mean of 4.3 hours. At the present time, the convective nature of the mesogranulation is still being discussed by different authors (Straus and Bonaccini 1997, Straus et al. 1992, Deubner 1989, Wang 1989). Although at the low photospheric levels, mesoscales appear as an extention of the granulation size without further distinction from granulation, they can be identified in the higher photosphere as internal gravity waves in the solar atmosphere (Straus and Bonaccini 1997). Various approaches to mesoscale measurement are necessary to understand their physical origin. The overlapping of mesogranulation and granulation and their respective evolutions (Darvann 1991) are the major difficulties in determining the mesoscale lifetime by indirect methods like the Local Correlation Technique (LCT). A long time sequence (of several hours) with subarcsecond spatial resolution, a large field of view and a quantitative mesocell definition are required for an accurate lifetime evaluation.

Send offprint requests to: Th. Roudier

The present investigation, using a 6.7 hour solar granulation time sequence obtained at the Pic du Midi Observatory, attempts to determine the lifetime of these mesocells. This is achieved by a direct measurement, following each cell from birth to death, and by the standard time correlation coefficient method.

2. Observations and reduction

The observations were obtained on August 17, 1990 at the "Turret Dome" of the Pic du Midi Observatory (France) in the quiet sun at the disk center. They consist in a 6 h 40 min time series (between 7:37 and 14:17 U.T.) of photosphere images in the CH band at 4308 Angs. (10 Angs. bandpass), where Network Bright Points are visible and may be used to delineate the supergranule cells. The exposure time on 1454 microfilm (35 mm) was 1/400 s. The time step of 45 seconds, which is the time delay used in the LCT algorithm, gives 533 frames for the entire sequence. The plate digitalization was performed with a MAMA microdensitomer (from the Institut National des Sciences de l'Univers in Paris). The digitization step was 40 microns, corresponding to a pixel size of $0.22''$. The final field of view, after alignment by cross-correlation, was $60'' \times 65.3''$. The images were not filtered to remove the 5 min oscillation.

Bogart et al. (1988) showed that good results can be obtained on large scale surface flows using the Local Correlation Technique (LCT) with a spatial resolution better than $1.5''$. Our data have a resolution lying between $0.25''$ to $0.5''$ during the entire sequence, which is good enough for flow computation. Horizontal velocities were determined by measuring the local displacements of the intensity field with gaussian masks of various sizes ($3.3''$ and $5.0''$, see below). The vectors of all the displacement fields were also averaged in different temporal windows (7 h , 1 h , 40 min, 20 min).

In Sect. 4, we used the 3-Hour time sequence previously analysed by Muller et al. (1992) for purpose of comparison.

3. Data reduction

Even though the solar granulation is directly visible on the sun's surface, the detection of the mesocell flows requires indirect methods such as the Local Correlation Technique (LCT) (cf. November, 1989). The use of such a method implies the careful adjustement of certain space and time parameters. Different LCT and feature tracking codes have been developed (Strous 1994, November 1988, Shine in Simon et al. 1988) in several institutes, and have recently been compared on the same data set (Simon at al. 1995). Particular care has to be applied to the selection of the pixel sizes with respect to the derived displacement between successive frames (Shine, Private communication 1997). An oversampling of the original data makes it possible to obtain reliable results, depending of the LCT method used, either an underestimate of flow velocities or excessive noise (Shine, private communication 1997). In our case, we used the LCT developed by L. November (1988), which is one of the methods suspected to underestimate flow velocities. The data pixel size of $0.22''$ seems to be a reasonable compromise for a time step of 45 seconds between successive frames, leading to shifts from one frame to the next of less than one pixel. In this case, the flows obtained by November's LCT are quite good (Simon, private communication 1997).

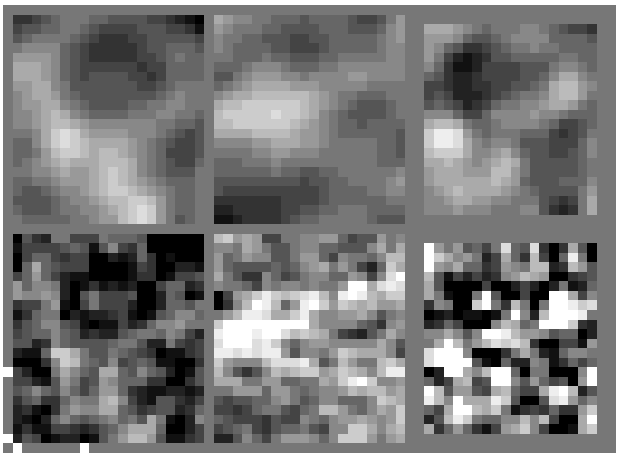

Fig. 1. Velocity components v_x,v_y and divergence maps (from right to left) calculated by the LCT algorithms of November (top) and Shine (bottom) with a temporal window of 40 min, a spatial window of $6.8''$ and a time delay of 45 s. White pixels in the v_x and v_y maps represent for positive velocities, while black pixels represent negative velocities. In the divergence maps (Fig. 1, right side, top and bottom), the positive divergence flows are white and the converging flows are dark. The field of view for v_x,v_y and the divergence maps is $60'' \times 65.2''$. The tick marks are $20''$ apart.

Horizontal flows have been computed by both LCT algorithms (November and Shine), on the same data set provided by our present observation. The same LCT parameters were selected in order to compare the flows: a time delay of 45 s., a spatial window of $6.8''$ and a temporal window of 40 min. Fig. 1 shows v_x,v_y and the divergence amplitudes of the flows as computed by both LCT algorithms from November (Fig. 1, top) and Shine (Fig. 1, bottom). In what follows, v_{xn},v_{yn} and divn represent the v_x and v_y components and the divergences calculated from November's LCT while v_{xs}, v_{ys} and divs represent the same components as calculated by Shine's LCT. Fig. 1 shows clearly that November's LCT algorithm tends to smooth flows when compared to the Shine's LCT algorithm although the same parameters have been used in the flow calculation.

Over the entire field of view, the correlation coefficients are found to be equal to: v_{ys} - v_{yn}: 65%, v_{xs} - v_{xn}: 56%, divs-divn: 63%. These correlation values increase up to 95% in well defined flows such as the divergence or convergence areas. A detailed inspection reveals smaller correlation in low velocity amplitude zones which are associated with the less well defined convergence area (Fig. 2a–d).

Fig. 2a shows the relative tilt angle between velocity vectors resulting from the two LCT algorithms (November and Shine), in diverging areas. These relative tilt angles are plotted with respect to the velocity modulus (taken as reference) calculated by Shine's LCT. The mean tilt angle is found to be 36°while the

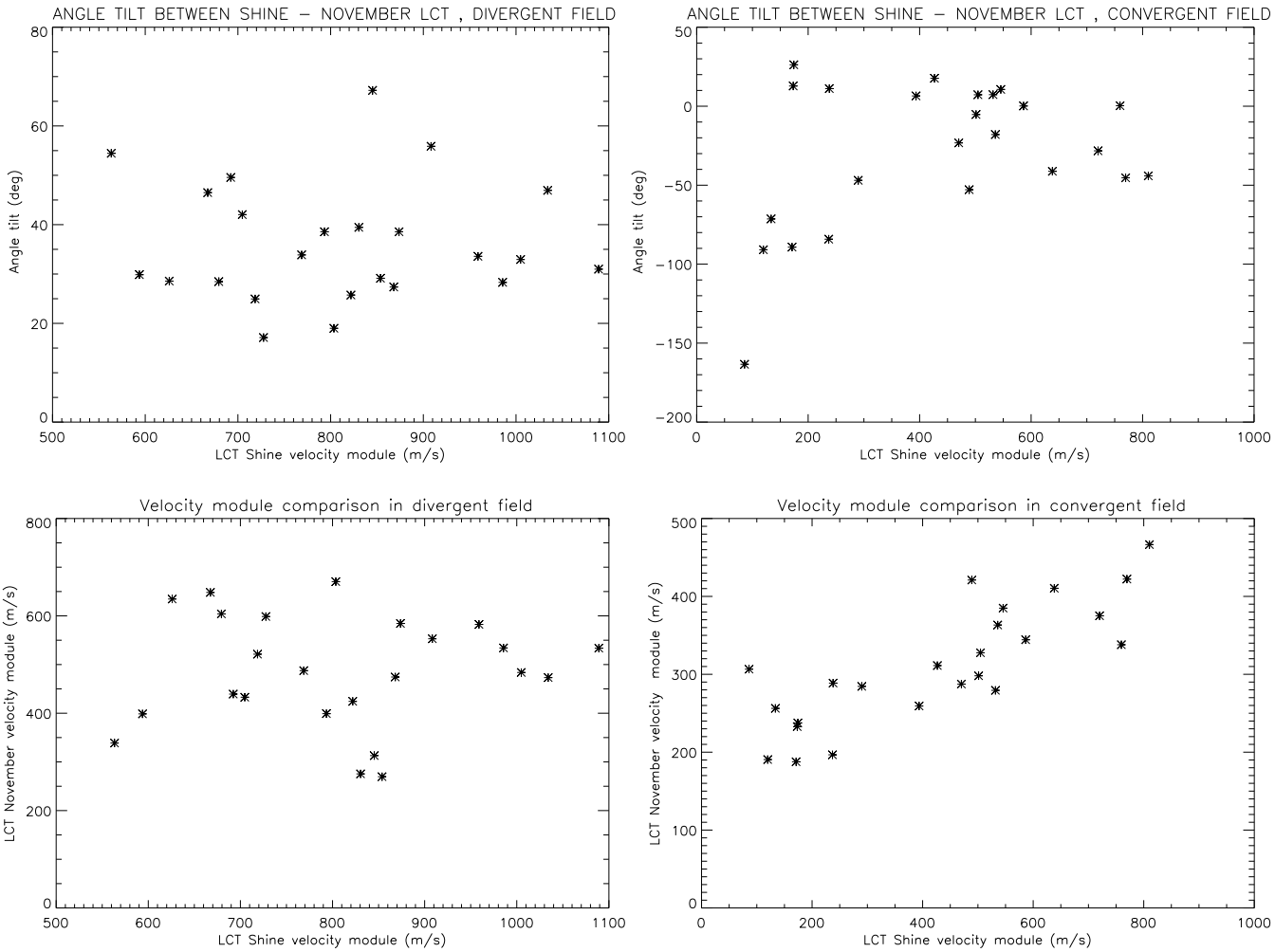

Fig. 2a–d. Plot of the moduli and the relative orientations of the flows vectors, as calculated by the two LCT algorithms (November and Shine), using the same reduction parameters: temporal window: 40 min., spatial window: 6.8″. **a** in the diverging flow region: relative tilt angle between flow vectors (November and Shine) versus the modulus of the velocity vectors as computed by Shine's LCT algorithm. **b** in the converging flow region: relative tilt angle between flow vectors (November and Shine) versus the modulus of velocity vectors as computed from Shine's LCT algorithm. **c** in diverging the flow region: modulus of the flow vectors as calculated by November's LCT algorithm versus the modulus of the flow vectors as calculated by Shine's LCT. **d** in converging flows region: modulus of the flow vectors as calculated by November's LCT algorithm versus the modulus of the flow vectors as calculated by Shine's LCT.

dispersion of the values is $\pm$ 20° around this mean regardless of whatever the velocity modulus.

Fig. 2b shows the relative tilt angle, as in Fig. 2a, but this time in converging flows. The degree of relative tilt angle dispersion is very high for velocities with amplitudes lower than 400 m/s. This tends to reduce the correlation coefficient on v_x and v_y components, as calculated by both LCT algorithms (November and Shine), over the entire field of view.

A comparison of the velocity vector moduli as calculated by the two LCT algorithms shows a linear correlation (slope = 0.3) of these moduli up to 700 m/s (Fig. 2c). Beyond this value, we detect an underestimation of the high velocity vector moduli in Fig. 2d (saturation effect) as computed by November's LCT with respect to the velocity vectors computed by Shine's LCT.

This underestimation is confirmed by a comparison of the histograms of v_{xs}, v_{ys} and v_{xn},v_{yn} components:

Shine	$-1100 < v_{xs} < 500$ m/s	$-500 < v_{ys} < 1000$ m/s
November	$-500 < v_{xn} < 500$ m/s	$-450 < v_{yn} < 450$ m/s

The divergence maps deduced from the flow calculated by both LCT algorithms (November and Shine) are quite similar in Fig. 1 (right side) as indicated by the correlation coefficient above. The differences between these two divergence maps are mainly the reinforced divergences in the Shine algorithm flows and the existence of one new small divergence in the Shine algorithm map (left corner) which is not present in the November algorithm map. These noise effects are due to both the saturation of the velocity amplitude in the November's LCT algorithm,

and to the relative tilt angle between the flows as calculated by November and Shine's algorithms.

From our detailed comparison of the flow as calculated by the two different LCT algorithms (November and Shine), we conclude that the flows are highly reliable except in regions where the flows have very small amplitudes and the vector orientations are determined with a large error. This tends more or less to reinforce some existent positive divergences and, in our case, to generate one small positive divergence which represents a difference of 5% in the number of the structures detected between these two approaches.

A quantitative determination of cell flow lifetime is commonly obtained by standard methods (temporal correlation, enumeration, etc...) which have been extensively discussed by Alisandrakis et al. (1987) and Title et al. (1989). For mesoscale flows, as in the case of granulation, cells split and suffer premature death when they collide with the supergranule boundaries,so that their intrinsic lifetimes may be somewhat longer (Muller et al. 1992). Nevertheless, the individual tracking and identification of divergence cells (mesoscales) are much easier than for granules. The divergence cells are well defined and few of them mix together or split. It has been estimated that 2 to 3% of the mesocells split during our sequence analysis. Unlike the case of solar granules, cell divergence does not develop from existing cell fragments, which make it easier to measure the lifetime of individual features by visual identification and in turn makes the results quite reliable.

The LCT method requires in particular the adjustment of two parameters, the temporal and spatial window sizes (L. November, 1988). The choice of temporal window depends on the phenomena, on which we would like to concentrate in our study (meso, super cells flow see Darwann 1991), and also on the oscillation, noise, and seeing filtering that we require. Early attempts used temporal window sizes of 20, 40 and 80 minutes to study the mesoscale properties in order to reduce the effect of the 5 min oscillations and seeing (L. November 1988, Darvann 1991, Muller et al. 1992). In the present study, we performed flow computation with 20, 40 and 60 minutes temporal window sizes. An FWHM applied to 3.3″ and 5″ gaussian window was used for the tracking.

4. Temporal behavior of the mesocells

The temporal properties of the mesocale flows were investigated using two different approaches:

1) temporal correlation coefficients applied to the v_x and v_y flow components.

2) identification and tracking of individual features in the divergence pattern.

4.1. Temporal correlation

Following the method used by Brandt et al. (1994), we characterize the mesoscale persistence by the temporal correlation coefficient, applied to the measured v_x and v_y flow components as obtained with the windows $<$ 40 min. $>$, 3.3″ and $<$ 60 min. $>$, 3.3″. As in Darvann (1991) and Brandt et al. (1994), we used the exponential form C(t)= C0 exp(-t/T) to get an 1/e decay estimation. Figs. 3a and b show, for each temporal window, the correlation coefficient "r" measured from various combinations of average flow maps as a function of the time difference between the maps. For example, the point at time difference = 10 min. in the Fig. 3 represents "r" measured between average flow maps no. 1 and 2, 2 and 3, 3 and 4, etc, and this for all the different time lags; the three plots in Fig. 3 represent the extrema (minima and maxima) and the average of the correlation coefficient values derived by this method.

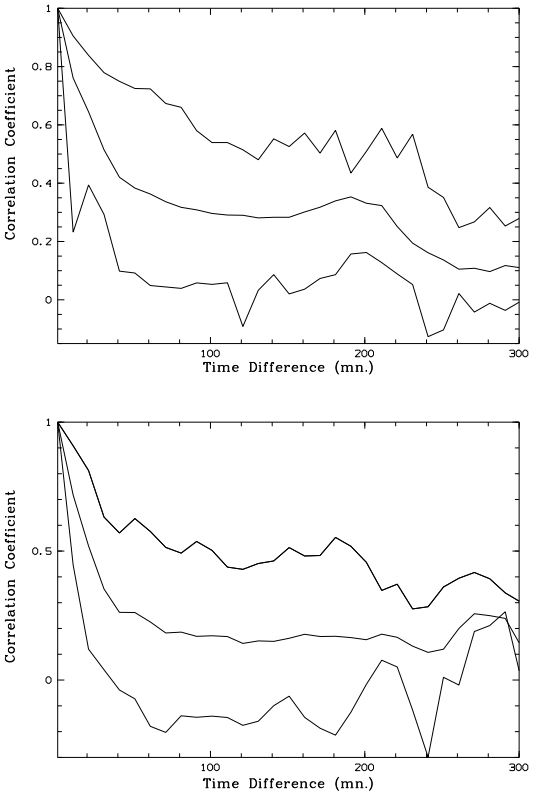

Fig. 3a and b. Decay of the correlation coefficient as a function of time for v_x **a** and v_y **b** components computed from a LCT temporal window of 40 min. and spatial window od 3.3″. The correlation coefficient were computed from various combinations of divergence maps as a function of the time difference between the maps (cf Darvann 1991 and the text). The middle line represents the mean correlation coefficient and the others two lines (top and bottom) are the extrema of the correlation coefficient.

In this correlation coefficient estimation, we selected the 40 and 60 minute temporal windows. This choice is a good compromise between the reduction of the seeing and granulation noise and the need to preserve of the intrinsic evolution of the flow pattern (see Brandt et al, 1994).

Taking, like Brandt et al. (1994), the highest values to represent the correlations which are less affected by residual seeing, we find a characteristic lifetime for T_{40} between 86–185 min and for T_{60} between 111–144 min. which is from 3 times to 40% less than the values previously obtained by the author cited

Table 1. Characteristic lifetime T deduced from the v_x and v_y flows gives, for two temporal windows 40 min. and 60 min and spatial window 3.3″.

Temporal window	Tmean (min.)	Tmax (min.)	Tmin (min.)	V component
40	48	185	30	v_x
40	36	86	15	v_y
60	74	144	40	v_x
60	63	111	38	v_y

above. The high scattering of the correlation coefficient values, as noted in Darvann (1991) and Brandt et al. (1994), is the major uncertainty in the estimation of mesogranulation lifetime by this method.

However, the means for T_{40} and T_{60} are found around 40 min. and 60 min. respectively, which indicates that the correlation technique is sensitive to the temporal window used in the LCT. This method is a global statistical approach in which the correlation coefficient is directly computed from frame to frame so that (v_x,v_y) are located at exactly the same (x,y) coordinates of the correlated sequence. Thus, it is natural that this method, computed over the entire field of view, should be affected by the temporal window. As will be shown below, directly tracking positive divergence by following the non negligible motions of the mesocell (in a small field) reduces influence of the temporal window (shape of the lifetime distribution) because of the cells' displacements. The v_x and v_y components which are indirectly correlated via the divergence values, are found at different locations (x0,y0),(x1,y1)....(xn,yn) during the mesocells' evolution, which tends to reduce the temporal window effects. The local proper evolution of the mesocells also reduces also these effects.

Thus, the correlation coefficient is representative of both the cells' lifetime and their proper motions.

4.2. Direct tracking

To study the temporal characteristics of the mesogranules, we computed the divergence from the horizontal flows. We define mesocells as the positive diverging flows. The temporal and spatial windows used in the present study help to prevent the generation of "artificial" divergence cells (with a scale of mesogranules), produced by strong gradients in the flows. The animated sequence of divergence maps when superposed on the granulation pattern, reveals granular explosion in the positive divergence corresponding to the existence of mesogranules. This increases our confidence in the use of the previous mesocell definition when studying their temporal properties. In order to monitor the persistence of the divergence cells as accurately as possible, a time step of 10 minutes between two consecutive divergence maps was selected. There is some flow pattern overlapping between successive divergence maps, but the experiment revealed that some features evolve independently of the temporal window sizes. The divergence maps of the flow field are made up of cells with a 4″–12″ diameter, whose divergences values are found to be around:

Table 2. Computed divergences using different averaging time and spatial windows.

Divergences (sec^{-1})	Temporal window (min.)	Spatial window (″)
$1.67\ 10^{-3}$	20	3.3
$4.17\ 10^{-4}$	40	3.3
$2.94\ 10^{-4}$	60	3.3
$4.43\ 10^{-4}$	40	5.0

The divergence values resulting from the 40 and 60 min temporal windows are commensurate with the previous results published by G. Simon et al. (1994). In the case of the 20 min temporal window, the divergence value appears sensitive to the granulation expansion. Darvann (1991) has demonstrated that granular evolution is the dominant noise source in the measurement of large scale flows. A rough estimation of the divergence for a symmetrical expansion <–. –> with a horizontal velocity of 1 km/s gives, in our case, a value of 6.2 10^{-3} sec^{-1}. Thus, the 20 min temporal window does not seem suitable for our purposes because of the influence of granule expansion. Darvann (1991) demonstrates that a considerable reduction of granular evolution noise may be achieved by averaging proper motion maps over an extended period. This explains the choice, in some previous papers, of studying mesocell properties with temporal windows greater than 40 min (see Brandt et al. 1994), as it makes it possible to sample as many granulation realizations as possible and then to reduce the granulation evolution noise.

Direct tracking of the cells during their evolution seems more suitable for our study. In order to track the cells during their life as accurately as possible, we focused our analysis on the three pairs of temporal and spatial windows given above. The divergence cell lifetime histograms are shown in Fig. 4 for two time sequences, 6 h 40 min and 3 h 00 min (Muller et al. observation 1992), resulting from flow computations with <20 min> and 3.3″ (FWHM) windows. The two graphs are quite similar in shape peaking around 30 min with a distribution reaching up to 2 h 20 min. This reveals the existence of a predominent component, probably due to the exploding granules (68% of cells with lifetime $\leq$ 50 min.), and of a flat component due to the mesoscale in the long lifetimes. Fig. 5 displays the cell lifetime histograms, for the < 40 min>, 3.3″, < 60 min>, 3.3″ and < 40 min>, 5.0″ windows. These distributions peak at around 30 to 40 min, with a respective maximum lifetime of 2 h20 min and 2 h 40 min. These graphs (and the associated integrated histograms), reveal that 70% of the cells have a lifetime $t \leq 50\,min$. The highest local maximun of the histogram (<60 min>,3.3″ pair) is probably a result of the convolution of the larger temporal window. In Fig. 5, the comparison between the cell lifetime histograms for the window pairs <40 min>, 3.3″ and < 40 min>, 5″ shows that, contrary to our expectation, an increase of the spatial window from 3.3″ to 5″ shifts the lifetime histograms to the smaller

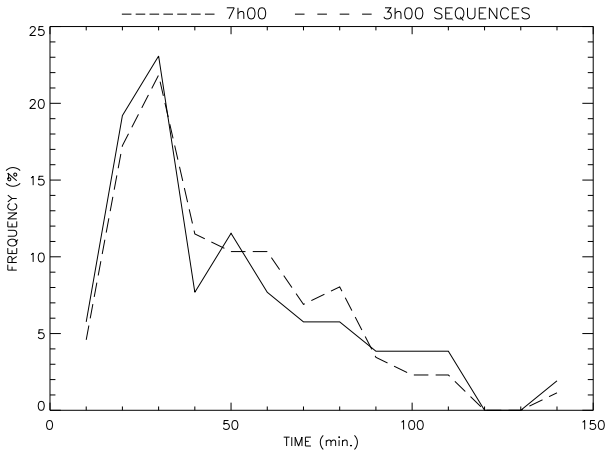

Fig. 4. Histograms of the Divergence cell lifetime measured from two different temporal series: the 6 h 40 min solar granulation sequence(observation described in this paper) and the 3 h 00 min solar granulation sequence previously described in (Muller et al. 1992). The flows derived from the two sequences have been determined by using L. November's LCT with a temporal window of <20 min> and a spatial window of 3.3″ (FWHM). The solid line represents the distribution of the divergence lifetime obtained from the 6 h 40 min sequence. The dashed line represents the distribution of the divergence lifetime obtained from the 3 h 00 min sequence.

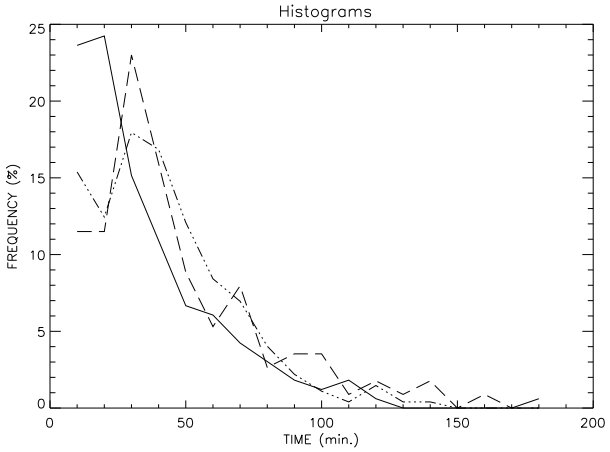

Fig. 5. Example illustrating the mesocell lifetime histograms obtained using different spatial and temporal windows. The abscissa is the time in minutes. The dotted line is the mesocell lifetime histogram for a temporal window of $<$ 40 min$>$ and a spatial window of 3.3″. The dashed line is the mesocell lifetime histogram for a temporal window of <60 min> and a spatial window of 3.3″. The solid line is the mesocell lifetime histogram for a temporal window of $<$ 40 min$>$ and a spatial window of 5.0″.

values on the abcissa. It seems that the larger size of the spatial window tends to smooth the effect of a greater number of granules with their proper motions. Thus, the combination of the granule evolutions and motions with a large window seems to reduce the measured cell lifetime.

We observe that, regardless of the spatial and temporal window sizes the positive divergences represent half of the field

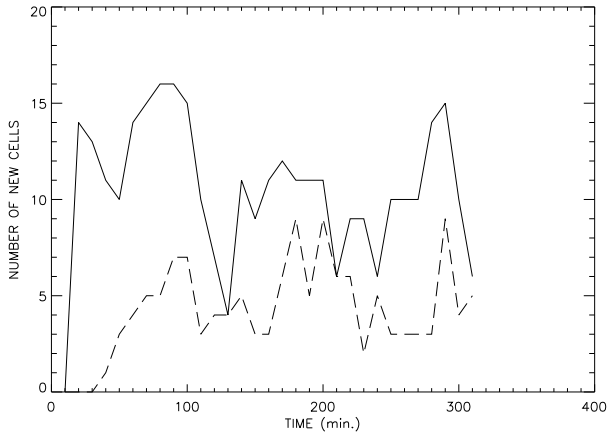

Fig. 6. Change in the number of new positive divergence cells in the field of view over time during the 6 h 40 min sequence. The solid line represents the number of new diverging cells obtained using the horizontal flows computed with the following LCT parameters: temporal window of $<$ 40 min$>$ and spatial window of 3.3″ The dashed line represents the number of new diverging cells obtained from the horizontal flows computed with the following LCT parameters: temporal window of <60 min> and spatial window of 3.3″

with a high stability (49% (σ = 1.5)%) during the entire time sequence (6 h 40 min). A surprising result concerns the change in the number of new positive divergence cells over time during our sequence. Indeed, this number varies with a period of 90 to 100 minutes, regardless of the spatial and temporal window sizes (Fig. 6). This variation is less marked for the $<$ 40 min.$>$,5.0″ pair. A verification of our data reduction process (alignment, filtering, LCT) revealed that it does not seem to produce a variation on such a time scale. It is thus like that this variation has probably a solar origin, but it has to be confirmed by another long time sequence.

The direct tracking method allows us to follow divergence cell motions with quite a high accuracy. Fig. 7 shows the measured displacements of the barycentre of cells with a lifetime $t \geq 70\,min$, over the solar surface. We observe more random mesocell motions in the supergranule than were observed by Muller et al. 1992. These motions do not seem to tend in any particular direction with respect to supergranule boundaries, which have been delineated by NPBs present in our observation and by the flow field averaged over 6 h 40 min (Fig. 8). The horizontal velocities deduced from these proper motions are represented in the histogram (Fig. 9). The values of horizontal mesocell velocity lie between 0.1 to 0.9 km/sec, with a peaked distribution at 0.5 km/sec, which is consistent with previous determinations (Muller et al. 1992, Brandt et al. 1988, Simon et al. 1994). The distance covered by cells during their lifetime is between 1 to 8″ (mean = 3.3″ (σ = 1.7″)) which corresponds to 25 to 50% of the cells' size.

5. Discussion

We have attempted in this paper to measure and quantify the lifetime of mesocells (4–10″) from a long time sequence

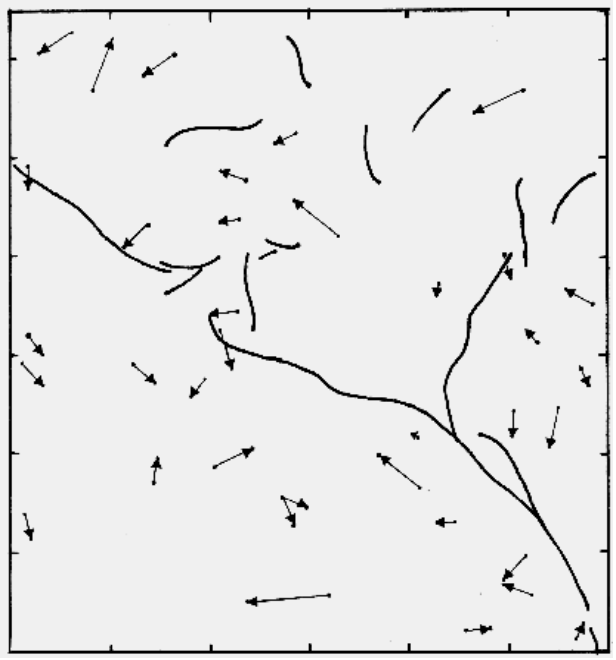

Fig. 7. Displacements, over the solar surface, of the barycenter for mesocells with a lifetime $t \geq 70\,min$. The tick marks are $10''$ apart. Supergranule boundaries have been delineated by the NPBs present in our observation during the sequence. Field of view: $60'' \times 65.3''$.

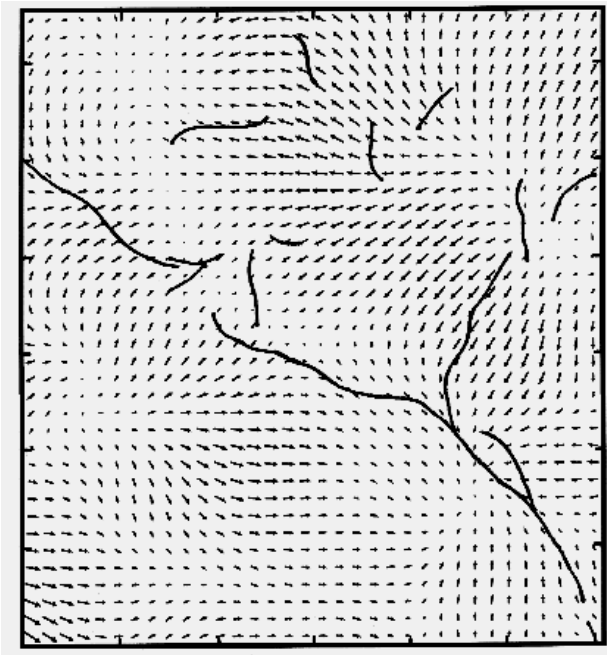

Fig. 8. Flow-field calculated by averaging the displacement vector over the entire 6 h 40 min sequence. Note the location of the NPBs present in our observation during the sequence (delineated by the solid line) most of which correspond to the converging flow of the supergranule. The tick marks are $10''$ apart. The total field of view is $60'' \times 65.3''$.

(6 h 40 min) obtained a the Pic du Midi Observatory. These mesocells were detected using the Local Correlation Technique (LCT) developed by L. November (1988). The adjustment of the pixel size with respect to the derived displacements and the comparison of horizontal flow measurements provided by the application of two different LCT algorithms (November 1988, Shine in Simon et al. 1988) to our data set make us confident in the reliablity of our results. We found that November's LCT, used in this study, underestimated high velocity flows when compared with Shine's LCT, but that the relative orientations and amplitudes of the velocity vectors are almost identical in most of the field of view, where the flows are well defined. The differences in the divergence maps derived by the two methods (November and Shine's LCTs) can be attribuated to a less accurate determination of the small velocities (moduli and orientations), in the less well defined convergent flows. Our detailed comparison of the flows calculated by both LCT algorithms (November and Shine) make us confident in the divergence locations and evolution.

Direct tracking of cells during their evolution seems to be a suitable method in order to monitor individual mesocells and quantify their lifetime.

The mesocell lifetime histograms derived from our measurements reveal a continuous distribution between 10 min and 2 h 40 min, peaked at around 30–40 minutes. This result is not significantly influenced by the choice of the temporal window in the LCT. 70% of the mesocells have a lifetime less than or equal to 50 minutes. Nevertheless, there is a clear component in the histogram which extends up to 2 h40 min, related to the long living mesoscale features. The short lifetime mesocell component is probably related to the family of exploding granules described by Kawagushi (1980). It could also represent the contribution of the exploders in the mesogranules, described by Simon et al. (1991), or else a component of scatterred exploding granules. From the continuous histograms of mesocell lifetimes, it is quite difficult to separate the granulation component from the mesogranulation component. Mesogranulation appears as an extended part of the granulation phenomena.

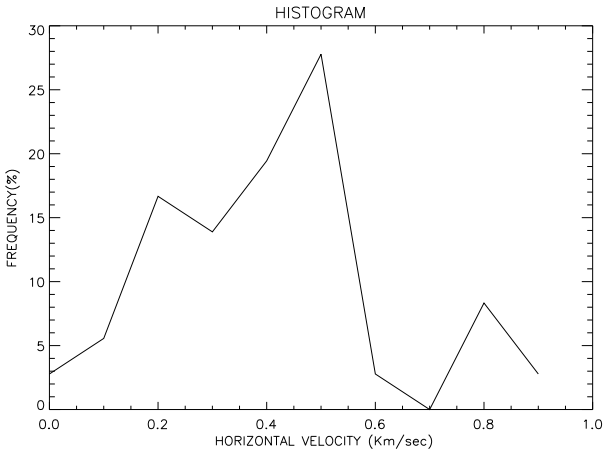

Fig. 9. Horizontal velocity histogram for mesocells with a lifetime $t \geq 70\,min$. These velocities are derived from the proper motions of these mesocells as shown in Fig. 7.

Mesocell lifetime has also been determined by the temporal correlation coefficient approach. This method, applied to the v_x and v_y flow components, yields results which are at least two to five times smaller than the previously published values (Brandt et al. 1994, Darvann 1991). The high scatter of the correlation coefficient values, described by Darvann (1991) and Brandt et al. (1994), is the major uncertainty in the determination of mesocell lifetime. Our observation was taken at higher altitude (40 km above $\tau = 1$) than the previous measurements, but we do not believe this factor could explain the differences. We think rather that the correlation coefficient method is too sensitive to the temporal window of the LCT and does not take into account proper mesocell motions.

Our estimation the mesocell lifetime is all smaller, by a factor 2 to 3, than Muller's observation (Muller et al. 1992). These differences may be explained by a mesocell selection arising from the use of a different definition, in particular for the direct measurement of lifetimes and motions. They only consider those divergences whose flows are circular around a central point while in the present study we use the divergence field which corresponds to an exploding activity.

We observe a variation in the number of new mesocells with a period of about 90–100 minutes, although the contribution of the positive divergences in the total field of view is quasi constant at 49% throughout the time sequence. This result does not seem to derive from our reduction method and, is likely to have a solar origin, but it has to be confirmed by other observations.

The measured horizontal velocity histogram of these mesoscale cells lies between 0.1 and 0.9 km/sec and peaks at 0.5 km/sec, which is commensurate with previous determinations (Muller et al. 1992, Brandt et al. 1988, Simon et al. 1994) In the previous determinations (Muller et al. 1992) mesogranule motions were observed to converge toward the supergranule boundaries with a mean velocity of 0.3–0.4 km/sec. In our sequence, the proper motions of mesogranules with a lifetime greater than or equal to 70 min seem more random than those described by Muller et al. 1992. The different organization of the proper mesocells motions as described by Muller et al. (1992) and by the present study can be attributed to the different locations of the mesocell field of view in the supergranular network. Muller's observation is centered on a supergranular cell while our study's field of view is located at the corner of 3 supergranular cells.

We conclude that mesocell lifetime determination yields disparities that can be attributed to the mesocell definition or to the method of flow measurement (LCT methods, temporal correlation, direct tracking, etc..). They may also be due to the different location of the observed field of view with respect to the supergranular network.

6. Conclusion

The important role played in the quiet sun by granules, supergranules and mesogranules has been studied and discussed extensively by Simon and Weiss (1989), Simon et al. (1991) and Brandt et al. (1994). Different kinematic approaches have been developed to match the observations to one another. More precisely, the simulation of the distribution of mesogranules and exploders has been studied with respect to supergranule cells.

For example, it has been found that the simulation of mesogranule cells centered at fixed points on a grid cannot collectively produce a supergranule velocity field (Simon et al. 1991). Proper supergranule horizontal flows are necessary in the simulations to reproduce the observations. Hence, mesogranules are considered to be independent features drifting with supergranular velocity (Simon et al. 1991) as was suggested by the Pic du Midi observations (Muller et al. 1992). Our results, with a longer time sequence (6 h 40 min) do not indicate such organized mesoscale motion over the solar surface. Indeed, our observation emphasizes to need for another approach to determine the relation between the different convection scales in the simulations.

The lifetimes and random proper motions of the mesocells analysed in the present study, have to be taken into account in the diffusion process which drags magnetics flux on the solar surface. The random walk of the magnetic flux tube,observed in the converging areas, is the result of the granular turbulence (Muller et al. 1992) but also of random, non negligible proper mesoscale motions, as described above. In particular, mesocell evolution (motions and morphology) certainly play a role in the constitution of the large-scale magnetic pattern in the quiet sun. It may also be suspected that an important role is being played by the mesoscale in the magnetic activity during the quiet sun's cycle. A precise measurement of the mesocale and flux tube transport properties provides a major challenge for the next five years.

Acknowledgements. We wish to thank Mrs M. Lafon for her technical assistance during this work. The photometric measurements were made with the "M.A.M.A." microdensitometer of the Institut National des Sciences de L'Univers in Paris. This work was supported by the Centre National de la Recherche Scientifique (C.N.R.S.) and by the Groupe de Recherche du CNRS "magnétodynamique solaire et stellaire". We would like also to thank Dr. R. Muller for many fruitful discussions. The authors wish to express their gratitude to L. November for providing his Local Correlation Tracking algorithm and for his valuable suggestions on using his software. We would like to give special thanks to R.A. Shine and Z. Frank (Lockheed, Palo Alto)for their assistance in providing LCT comparisons between the different techniques; to Drs P.N. Brandt (KIS institut, Germany) and G.W. Simon (Sacramento Peak, USA) for their comments and recommendations concerning the use of LCT technique; and to the referee for his helpful suggestions on how to clarify the text.

References

Alisandrakis C.E, Dialetis D. and Tsiropoula 1987, A&A 174, 275
Andersen B.N., Leifsen T., Toutain T., 1994, Solar Phys. 152 247
Bogart R.S., Fergusson,S.H., Scherrer, P.H., Tarbell, T.D., Title, A.M,: 1988 Solar Phys. 116, 205
Brandt P.N., Scharmer G.B.,Ferguson S., Shine R. A., Tarbell T.D., Title, A.M. 1988, Nature 335,238
Brandt P.N., Ferguson S., Scharmer G.B., Shine R. A., Tarbell T.D., Title, A.M. and Topka K., 1991 A&A 241,219

Brandt P.N., Rutten R.J., R.A. Shine and Trujillo Bueno 1994 in R.J. Rutten and C.J. Schriver (eds), Solar surface Magnetism,251,259 Kluwer Ac. Publ.
Darvann 1991 Thesis, University Oslo
Deubner 1989 A&A vol 216, n1-2, 259
Kawagushi I. Solar Phys. 1980 65,207
Küveler, G.,: 1983, Solar Phys. 88, 13
Leighton, R.B., Noyes, R. W., Simon, G.W., 1962, ApJ. 135, 474
November L.J., Toomre J., Gebbie K. and G. Simon, 1981, ApJ 245, L123-L126
November L.J., Toomre J., Gebbie K. and G. Simon 1982, ApJ 258, 846
November L.J. 1989,p. 457,in High Spatial Resolution Observations, O. Von der Lühe (ed.), Sunspot, N.M., p. 457
Muller, R., Auffret, H., Roudier, Th., Vigneau, J., Simon, G.W., Frank, Z., Shine, R.A., Title, A., 1992 Nature Vol 356, 322.
Rabello Soares M.C., Roca Cortés T., Jiménez A., Andersen B.N. and Appourchaux, 1997, A&A 318, 970.
Simon, G.W. and Leighton, R.B., 1964 ApJ, 140, 1120
Simon, G.W., Title, A.M., Topka, K.P., Tarbell, T.D., Shine, R.A., Ferguson, S.H., Zirin, H., and the SOUP Team: 1988 ApJ 327, 964
Simon G.W. and Weiss N.O. 1989, ApJ 345, 1060
Simon G.W., Title A.M. and Weiss N.O. 1991, ApJ 375, 775
Simon G.W., Brandt P.N., November J.L, Scharmer G.B. and Shine R.A, 1994, in R.J. Rutten and C.J. Schriver (eds), Solar surface Magnetism, Kluwer Ac. Publ.
Straus and Bonaccini 1997 *A&A*, in press
Straus Th, Deubner F.L., Fleck B., 1992, A&A 256, 652
Strous L. 1994 Thesis, University Utrecht
Title, A.M., Tarbell T.D., Topka K.,Ferguson S. and Shine RA., 1989, ApJ 336, 475.
Wang H., 1989, Solar Phys. 123, 21

This article was processed by the author using Springer-Verlag LaTeX A&A style file *L-AA* version 3.